

## Experimental Study of Bubble Detection in Liquid Metal

R. Guichou, P. Tordjeman, W. Bergez, R. Zamansky, K. Paumel

### Abstract

Bubble detection in liquid metal is an important issue for various technological applications. For instance, in the framework of Sodium Fast Reactors conception, the presence of gas in the sodium flow of the primary and secondary loops is a problematic of crucial importance for surety and reliability. Here, the two main measurement methods of gas in sodium are Ultrasonic testing and Eddy-current testing; we investigate the second method in our study. In a first approach, we have performed experiments with liquid metal – galinstan – containing insulating spherical beads of millimeter order. The liquid metal is probed with an Eddy-current Flowmeter (ECFM) in order to detect the beads, and characterize their diameter and position. Results show that the signal measured by the ECFM is correlated to the effect of these parameters. Finally, an analytical model is proposed and compared to the experimental results.

### Introduction

Bubble detection and characterization in opaque media such as liquid metals is a still unsolved subject of research, which finds applications in several industrial domains, from the nuclear energy – in the Sodium Fast Reactors (SFR) – to the metallurgy. In the SFRs, the liquid sodium is used as a coolant of the nuclear core, and the presence of bubbles in the flow can disrupt the cooling properties of the liquid and also the neutron scattering of the core. Due to the physical properties of sodium, two measurement methods distinguish themselves for the gas detection: Eddy-current method, which is the principle we investigated, and Ultrasonic testing. Eddy-current testing is commonly used for detection of superficial defects in metallic bodies. Besides, flowmetry with Eddy-currents has already been implemented successfully for various liquid metals [1] [2].

The main objective of the study is to have a robust method to detect inclusions, such as bubbles or impurities, in liquid metals with the aid of an Eddy-current Flowmeter (ECFM). In this paper, we also present models that have been developed to understand and analyze the measured signals. These models are based on a perturbative approach of the magnetic flux due to the two-phase liquid metal at low magnetic Reynolds numbers ( $Re_m \ll 1$ ) and small skin depths,  $\delta \ll D$  where  $D$  is the characteristic length of the flow. A perturbative model has already been developed in [3]. It states that the total magnetic flux  $\phi$  in the two-phase liquid can be expanded at first order in flow speed  $U$  and void fraction  $\alpha$  :  $\phi \approx \phi_0 + \phi_U + \phi_\alpha$ , where  $\phi_0$  is the flux in the absence of motion and due to Faraday effects,  $\phi_U$  is the flux due to motion effects and  $\phi_\alpha$  is the perturbation of the flux due to the dispersed phase.

In the first part, we present the experimental set-up consisting of a tube of liquid metal (galinstan) containing insulating beads arranged in known position and diameter. An ECFM translates along the tube to probe the liquid metal. The frequency range of the current supplying the ECFM is between 1000 Hz and 3000 Hz ( $Re_m \ll 1$  and  $4.8 < \delta < 8.3$  mm). In the second part, we study the ECFM response, by varying the current frequency  $f$ , the ECFM speed  $U$  and

the bead diameter  $D$  (bead position fixed). In the third part, we propose an analytical model of the perturbation of the magnetic field by one bead, and compare it with the experimental results.

## 1. Experimental Set-Up

The set-up (Fig 2 Fig 1) consists of a vertical tube made of non-conductive non-ferromagnetic Macor ceramic tube (inner diameter 25 mm, outer diameter 29 mm) containing a static two-phase liquid metal : galinstan (alloy of Gallium, Indium and Tin). Spherical beads made of polymer material by 3D printing are disposed in galinstan (with four diameters: 2, 3, 4 and 5 mm). The radial position of the beads is fixed with a thread at three different distances from the axis of the tube (3.5, 6.5 or 9.5 mm). Each tube contains one thread at a given position on which two beads of different diameter are stuck at a distance of 90 mm one to the other, in order to avoid overlap effect on the ECFM signal. A control tube containing only galinstan is used as a reference to enlighten the influence of the beads on the measures.

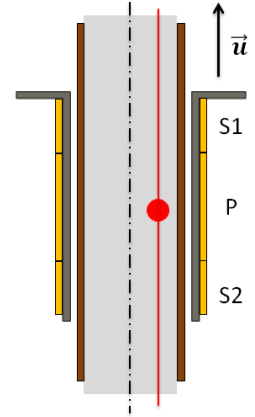


Fig 1. Explanatory layout

The ECFM is composed of 3 coaxial coils mounted on a PEEK polymer ring (inner diameter 31 mm, outer diameter 35 mm) : a primary coil P (length 20 mm, inner diameter 35 mm) and two secondary coils  $S_1$  and  $S_2$  (length 10 mm, diameter 35 mm) on either sides (Fig 1). Each coil is composed of two layers of winding (copper wire of diameter 0.6 mm).

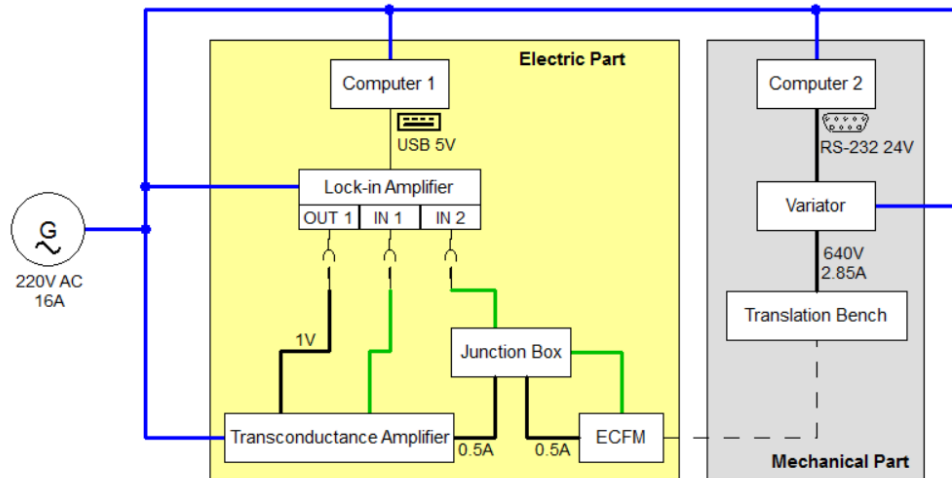


Fig 2. Functionnal scheme of the experimental set-up

The ECFM is fixed to an uniaxial displacement controller – piloted by the computer 2 – and translates vertically along the tube at speeds from 1 mm/s to 1000 mm/s. Hence (by referential change), the ECFM probes a two-phase plug-flow. For each measurement, the ECFM is translated back and forth several times.

A lock-in amplifier piloted by the computer 1 (Fig 2) generates AC signals of given frequency (1000 to 3000 Hz) and voltage (1 V). The transconductance amplifier produces an AC output current  $i_0$  of constant amplitude (0.5 A) supplied to the primary coil P. The generated magnetic field produced by P induces eddy currents inside the galinstan, whose distribution is modified by the motion of the liquid metal and the presence of the insulating beads. The total magnetic flux induces an e.m.f. in secondary coils  $S_1$  and  $S_2$ . The voltage difference  $\Delta V = V_{S_2} - V_{S_1}$  between the two secondary coils is measured and amplitude-demodulated by the lock-in

amplifier with  $i_0$  as phase reference. We note the in-phase component  $\Delta V_{\parallel}$  and the quadrature component  $\Delta V_{\perp}$ . We note  $|\Delta V| = \sqrt{(\Delta V_{\parallel})^2 + (\Delta V_{\perp})^2}$  and the phase  $\theta = \tan^{-1}(\Delta V_{\perp}/\Delta V_{\parallel})$ .

## 2. Experimental results

Typical demodulated signals of the ECFM are depicted in Fig 3 where the bead diameters are 4 and 5 mm and the current frequency is 2000 Hz, for the whole speed range. The ECFM position coordinate corresponds to the middle of the middle of the primary coil. The measured voltage is the voltage difference between the two secondary coils (in-phase and quadrature components). The reproductivity of the results has been tested by measuring the signal for several translations of the ECFM and the mean standard deviation is below  $2 \mu\text{V}$ , which is much smaller than  $\Delta V$  ( $\sim 1 \text{ mV}$ ).

At 1 mm/s and without bead, induction due to motion is negligible and we have  $\Delta V_{\parallel} \approx \Delta V_{0,\parallel}$  and  $\Delta V_{\perp} \approx \Delta V_{0,\perp}$ . It can be noticed that  $\Delta V_{0,\parallel}$  and  $\Delta V_{0,\perp}$  should be zero for an ideal ECFM. The Lorentz induction in the galinstan, due to its motion, manifests itself in two offsets  $\Delta V_{U,\parallel}$  and  $\Delta V_{U,\perp}$ . The presence of the two beads manifests itself by two oscillations of amplitudes  $\Delta V_{\alpha,\parallel}$  and  $\Delta V_{\alpha,\perp}$  centered on the bead position (46 mm and 136 mm for 5 mm bead and 4 mm bead respectively).

Fig 4 depicts the variations of  $|\Delta V_U|$  and  $\theta_U$  versus ECFM speed for the tube without beads. The module  $\Delta V_U$  varies linearly with speed, which is in agreement with [3]. The phase  $\theta_U$  is invariant for velocity larger than 20 mm/s. For velocity smaller than this value, the voltage offset measurement is subject to larger uncertainties due to its small value.

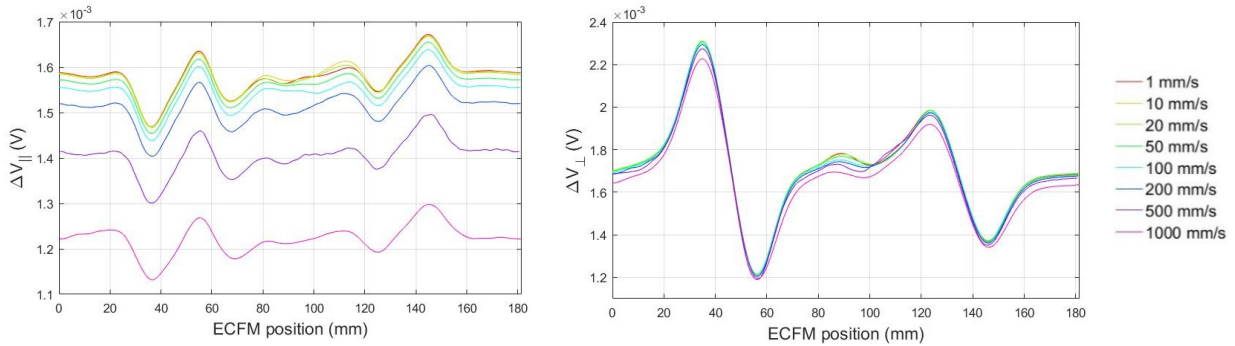


Fig 3. Demodulated signal (In-phase and quadrature components) (2000 Hz, radial position  $r = 9.5 \text{ mm}$ )

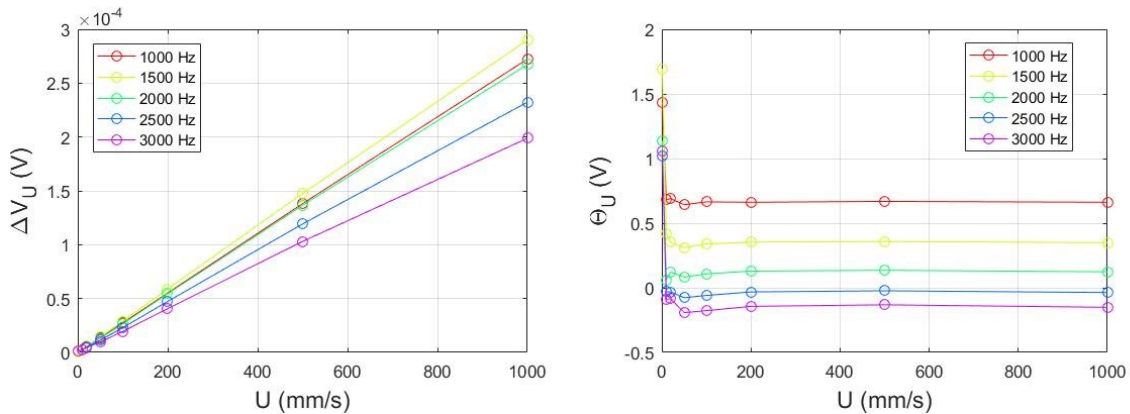


Fig 4.  $\Delta V_U$  and  $\theta_U$  vs. ECFM speed  $U$

The effect of frequency is shown in Fig 5 for the same tube. The module increases with  $f$  up to a maximum occurring at 2000 Hz independent of the velocity. The phase  $\theta_U$  decreases monotonically with frequency and becomes negative at  $\sim 2400$  Hz for the whole range of velocity. These effect is strongly dependent on the electrical conductivity of the metal, and the change of sign does not occur for solid aluminium which is consistent with [3].

The bead effects are presented in Fig 6 to Fig 8. Fig 6 depicts  $\Delta V_\alpha$  and  $\theta_\alpha$  versus speed  $U$  for a bead of diameter 5 mm. As in [3], we observe that  $\Delta V_\alpha$  and  $\theta_\alpha$  approximately do not depend on velocity. This result is fundamental to decouple velocity effects and void fraction effects and is the basis for bubble detection [3]. On the contrary, the oscillation amplitude depends strongly on frequency as it is shown in Fig 7 for a velocity of 1 mm/s. As the frequency rises,  $\Delta V_\alpha$  increases as a consequence of the intensification of the current density in galinstan (Faraday induction law). On the other hand,  $\theta_\alpha$  decreases with frequency for the whole range of bead diameters.

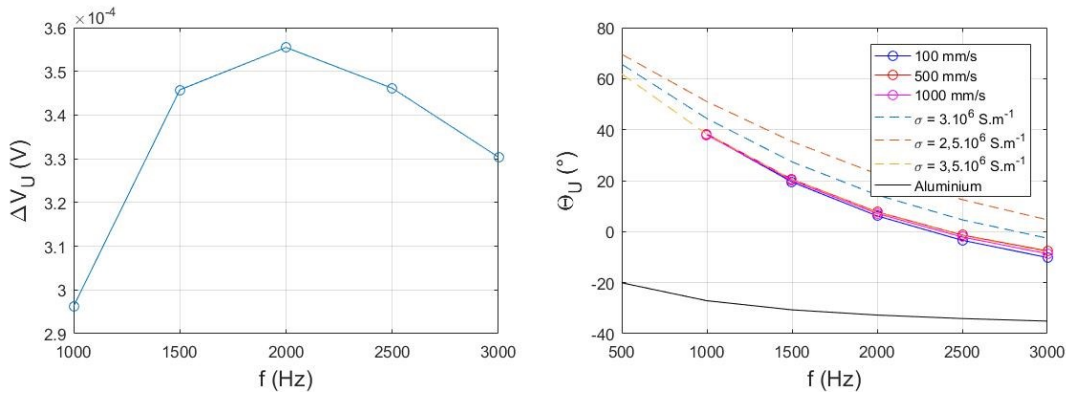


Fig 5.  $\Delta V_U$  and  $\theta_U$  vs. frequency  $f$

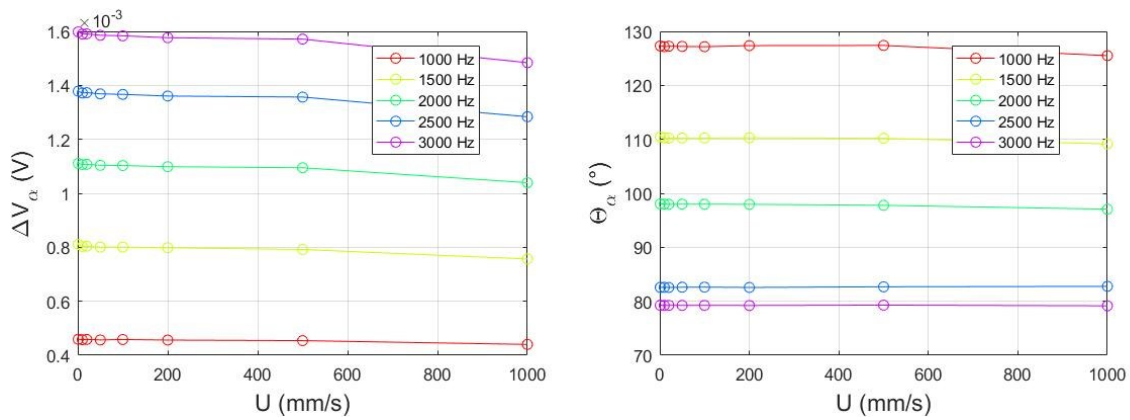


Fig 6.  $\Delta V_\alpha$  and  $\theta_\alpha$  vs. ECFM speed  $U$

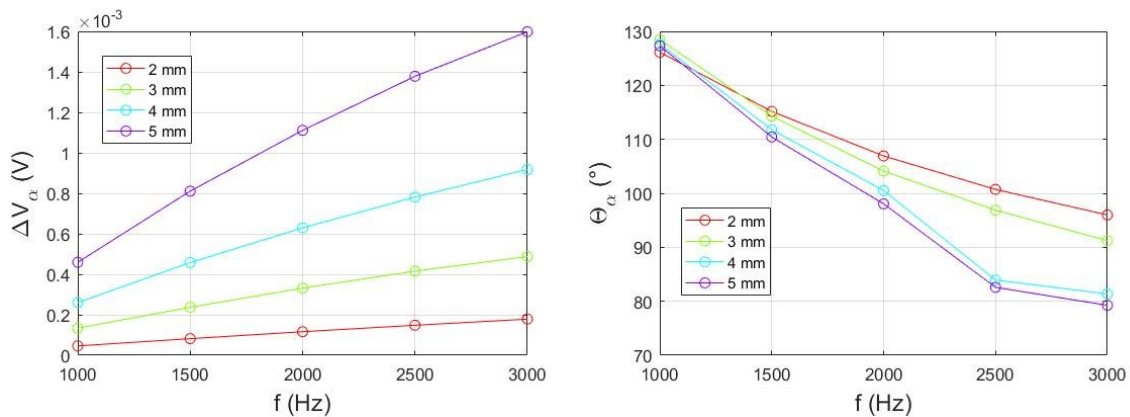


Fig 7.  $\Delta V_\alpha$  and  $\theta_\alpha$  vs. frequency  $f$

Fig 8 depicts  $\Delta V_\alpha$  and  $\theta_\alpha$  of the oscillation amplitude versus bead volume for a velocity of 1 mm/s.  $\Delta V_\alpha$  increases with the volume of the bead. The phase  $\theta_\alpha$  of the oscillation decreases as the bead volume increases, and this decrease is even more important as the frequency increases.

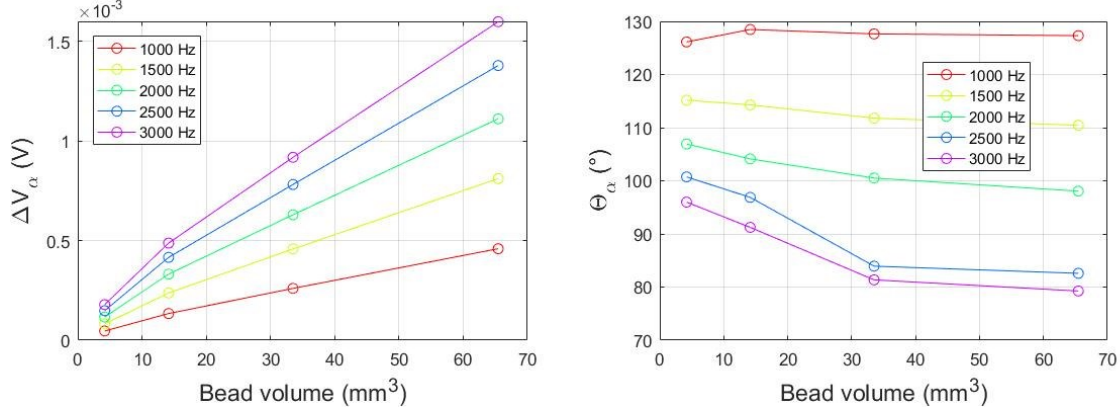


Fig 8.  $\Delta V_\alpha$  and  $\theta_\alpha$  vs. bead volume  $\pi D^3/6 (G_3^D P_1^f)$

### 3. Discussion

The analytical solution of a coil surrounding a metal cylinder [4] is extended in this study to the case of a coil crossed by liquid metal (single phase) in motion. The induction equation of the vector potential  $\mathbf{A}$  in the metal is given by:

$$\frac{\partial \mathbf{A}}{\partial t} = \frac{1}{\mu\sigma} \nabla^2 \mathbf{A} + \mathbf{u} \times (\nabla \times \mathbf{A}), \quad (1)$$

where  $\mu$  is the vacuum permeability and  $\sigma$  the electrical conductivity of the metal.

The Fourier transform of this equation in cylindrical coordinates lead to:

$$\frac{\partial^2 \tilde{\mathbf{A}}}{\partial r^2} + \frac{1}{r} \frac{\partial \tilde{\mathbf{A}}}{\partial r} - \frac{\tilde{\mathbf{A}}}{r^2} - (2\pi\zeta)^2 \tilde{\mathbf{A}} + j(2\pi\zeta)\mu\sigma u \tilde{\mathbf{A}} - j\omega\mu\sigma \tilde{\mathbf{A}} = 0, \quad (2)$$

where  $\zeta$  is the spatial frequency and  $\omega$  the pulsation.

This equation shows that Faraday induction ( $-j\omega\mu\sigma \tilde{\mathbf{A}}$  in Equation (2)) and Lorentz induction ( $j(2\pi\zeta)\mu\sigma u \tilde{\mathbf{A}}$  in Equation (2)) are responsible of the phaseshift of Fig 5. The ratio of the Lorentz induction term and the Faraday induction term being proportional to the magnetic Reynolds number (much lower than 1), the Lorentz induction plays barely on the phaseshift. This explains why  $\theta_U$  is not dependent on the speed in Fig 4 and Fig 5. Moreover, the lower the frequency, the lower the Faraday induction and the lower the phaseshift (with regard to the reference signal). The reference signal (current in primary coil) being a sine, the phaseshift  $\theta_U$  shall equal to  $90^\circ$  as the frequency tends towards zero, which seems to be the case in experimental results (up to the limit of the frequency range).

To account for the effect of the bead, we propose to modelize its presence by a magnetic dipole oriented along the  $z$  axis. The magnetic moment  $m$  (Equation (3)) is function of the parameters  $D$ ,  $h$  and  $f$  in the first hand, and of the spatial distribution of the current density in the metal (known by the analytical solution) in the second hand.

$$m(z) = C(D, h, f) \sqrt{\frac{j(z)}{j(z=0)}} \quad (3)$$

Fig 9 shows the perturbation observed in the measured signal and the perturbation due to the magnetic dipole for a bead of diameter 5 mm, at a speed of 1 mm/s, at a frequency of 1000 Hz (left) and 2000 Hz (right). The model appears to be in good agreement with the experimental result.

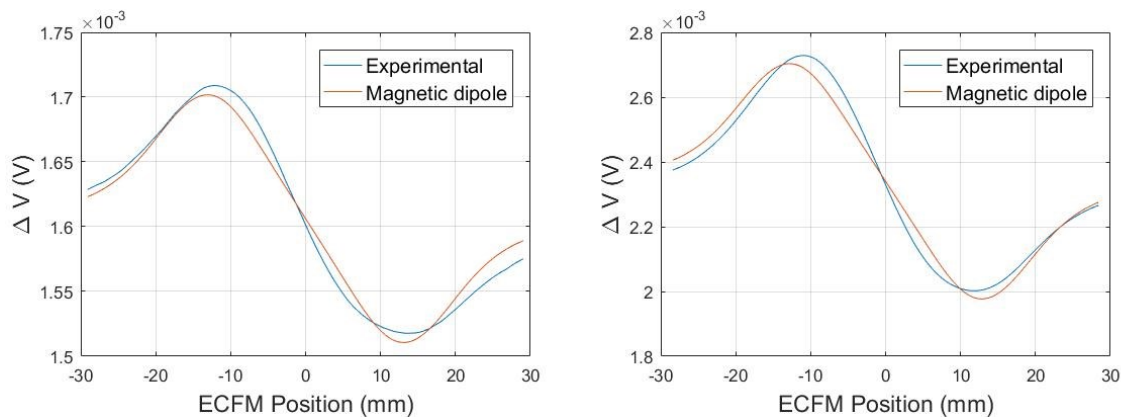


Fig 9. Perturbations observed for a bead of 5 mm, at 1 mm/s, at 1000 Hz (left) and 2000 Hz (right)

## Conclusions

In this paper, the ability of an Eddy-current Flowmeter (ECFM) to detect an inclusion – in the form of an insulating bead – inside a liquid metal has been attested by the experiment. A parametric study has been performed varying the size of the inclusion, the excitation frequency of the ECFM, and the relative motion of the liquid metal to the ECFM. The signal response to the motion follow a linear trend versus speed – which is in agreement with the literature and the analytical solution. The signal response to the passing of a bead appears to be invariant versus speed but highly dependent versus frequency and inclusion size. A descriptive model has been developed and confronted with the experimental results. A second model is under preparation in order to have a physical explanation of the inclusion perturbation.

## References

- [1] M.Kumar, W.Bergez, Ph.Tordjeman, R.Arinerio et K.Paumel, «Magnetic flux distortion in two-phase liquid metal flow: Model experiment,» *Journal of Applied Physics*, vol. 119, n° 118, 2016.
- [2] C.C.Dodd et W.E.Deeds, «Analytical Solutions to Eddy-Current Probe Coil Problems,» *Journal of Applied Physics*, vol. 39, n° 12829, 1968.
- [3] S.Sureshkumar, M. Sabih, S.Narmadha, N.Ravichandran, R.Dhanasekharan, C.Meikandamurthy, G.Padmakumar, R.Vijayashree, V.Prakash et K.K.Rajan, «Utilization of eddy current flow meter for sodium flow measurement in FBRs,» *Nuclear Engineering and Design*, vol. 265, pp. 1223-1231, 2013.
- [4] R. C. Baker, «Electromagnetic Flowmeters for Fast Reactors,» *Progress in Nuclear Energy*, vol. 1, pp. 41-61, 1977.

## Authors

Guichou, Rafael Tordjeman, Philippe  
 rguichou@imft.fr philippe.tordjeman@imft.fr  
 Institute of Fluid Mechanics (Toulouse), France

Bergez, Wladimir  
 wladimir.bergez@enseeiht.fr

Zamansky, Rémi  
 remi.zamansky@imft.fr